Hindawi
Advances in Civil Engineering
Volume 2023, Article ID 5547591, 12 pages
https://doi.org/10.1155/2023/5547591

Research Article

Properties of Carbonated Steel Slag Admixture in the Cementitious System

Lie Sun,[1] Hui Wang,[2] and Yali Wang[1]

[1]*Faculty of Materials and Manufacturing, Beijing University of Technology, Beijing, China*
[2]*State Key Laboratory of Solid Waste Reuse for Building Materials, Beijing Building Materials Academy of Science Research, Beijing, China*

Correspondence should be addressed to Yali Wang; wangyali1978@bjut.edu.cn

Received 20 June 2023; Revised 6 October 2023; Accepted 8 November 2023; Published 8 December 2023

Academic Editor: Junqing Zuo

Global warming caused by carbon dioxide (CO_2) emissions has emerged as an undeniable environmental concern. While advocating for energy conservation and emissions reduction, the challenge of addressing the substantial CO_2 emissions cannot be underestimated. Currently, steel slag is utilized in carbon capture and storage technology due to its potential for carbonation. However, the carbonation of steel slag necessitates a stable and cost-effective carbon source. Industrial exhaust gases are considered a viable option, but they often have low CO_2 concentrations, resulting in sluggish carbonation rates. Therefore, this study focuses on directly converting steel slag powder into concrete mineral admixtures to enhance the carbonation rate at low CO_2 concentrations. Experimental results reveal that a carbonation time of 3–7 days, a liquid–solid ratio of 50%, and the selection of sodium silicate as the alkali activator yield the optimal carbonation conditions. Under these conditions, the CO_2 uptake can reach 15.3%–16.0%, and the f-CaO content can be reduced to 0.2%–0.3%. Mixing 30% carbonated steel slag powder with P·I 42.5 cement in mortar samples yields a compressive strength of 32.1 MPa at 7 days and 47.5 MPa at 28 days, along with a flexural strength of 6.2 MPa at 7 days and 8.0 MPa at 28 days. The addition of carbonated steel slag powder not only enhances the mechanical properties but also reduces the pore diameter in the hardened cementitious system. In 7 days, the pore size decreases from being concentrated around 349 nm to approximately 282 nm, and in 28 days, the pore size decreases from being concentrated around 62 nm to roughly 55 nm. This transformation is primarily attributed to the role played by calcite grains in the carbonated steel slag powder, which facilitates nucleation and filling effects.

1. Introduction

Global warming is primarily caused by greenhouse gases such as carbon dioxide (CO_2), methane (CH_4), and nitrogen oxide (N_2O) [1]. Among these, CO_2 is the most significant. The environmental issue of global warming stemming from CO_2 emissions cannot be underestimated. Currently, various methods have been developed to mitigate CO_2 emissions into the atmosphere, with carbon capture and storage (CCS) technology being considered the most promising approach [2]. CCS technology is a critical means of addressing CO_2 emissions, and without it, the cost of achieving a 0.45‰ CO_2 equivalent reduction by 2,050 would increase by 138% [3]. Viable CCS technologies to date include geological storage, ocean storage, biological storage, and mineral storage. Mineral sequestration is regarded as the safest method for CO_2 sequestration, offering a high storage capacity (1 trillion tons of CO_2) and the potential to store all future emissions [4].

Numerous industrial waste slags are widely employed in CO_2 storage. In comparison to raw ores, industrial waste slag is not only readily available but also cost effective. Currently available industrial waste slag includes blast furnace slag [5], fly ash [6], and steel slag. Meanwhile, China, with its rapidly expanding steel industry, has become the world's largest steel consumer, accounting for 50% of global crude steel production [7]. In 2019, China's crude steel production reached 996.3 million tons, generating nearly 150 million tons of steel slag. However, the comprehensive utilization rate of steel slag in China stands at only 30%, significantly lower than the 85% rate achieved in many developed countries. A substantial

amount of steel slag is improperly stored and landfilled, resulting in severe environmental and social hazards [8].

Steel slag shares chemical and mineral compositions similar to cement, making it a potential candidate for carbonation [9, 10]. The chemical composition of steel slag predominantly comprises CaO (45%–60%), SiO_2 (10%–15%), Al_2O_3 (1%–5%), Fe_2O_3 (3%–9%), MgO (3%–13%), FeO (7%–20%), and P_2O_5 (1%–4%). These oxides are primarily present in steel slag in mineral forms, including C_3S, C_2S, and the RO phase (a continuous solid solution composed of MgO, FeO, and MnO) [11]. Notably, f-CaO, f-MgO, C_3S, and C_2S can all react with CO_2 during carbonation.

Furthermore, China has set long-term goals of achieving a peak in carbon emissions by 2030 and carbon neutrality by 2060. To attain these objectives, industries are actively seeking emission reduction strategies. Among these, the cement industry contributes 8% to global CO_2 emissions, with China's cement clinker production accounting for roughly 60% of the world's output [12]. Consequently, there is a pressing need to identify new-generation low-carbon cementitious materials to replace conventional cement. Given the challenges associated with CO_2 emissions and steel slag reuse, the carbonation of steel slag to produce cementitious materials offers a viable solution.

Carbonating steel slag has several advantages, including the reduction of carbon emissions, resolution of CO_2 emission challenges, improved stability of steel slag in construction applications [13], and early strength enhancement [14]. Owing to its complex mineral composition, steel slag contains significant amounts of f-CaO and f-MgO in addition to its primary components such as C_3S and C_2S. These substances contribute to volume stability issues in cementitious systems, a critical concern in steel slag applications. The f-CaO in steel slag is not only abundant but is often encapsulated within C_2S [15], rendering it inaccessible. Carbonation of steel slag consumes C_2S, allowing for the utilization of f-CaO. Consequently, carbonation effectively removes f-CaO and f-MgO, facilitating the extensive use of steel slag in construction projects. As a cementitious material, steel slag typically exhibits low early stage strength due to the relatively high C_2S content and slow hydration rate. However, carbonation converts C_2S into calcium carbonate ($CaCO_3$), and the microhardness of $CaCO_3$ (calcite) is approximately 5–5.5 GPa [16], effectively improving early stage strength. In addition, in cementitious systems, carbonation of steel slag promotes a dense structure and enhances durability, including improvements in volume shrinkage [17] and freeze–thaw resistance [18]. In summary, the carbonation of steel slag holds significant application potential.

To date, scholars have explored various methods to carbonate steel slag and convert it into building materials such as mineral admixtures [19], bricks [20], and aggregates [21], yielding valuable results. However, several unresolved issues persist. First, most researchers have employed high-temperature, high-pressure, and high-concentration conditions for the carbonation of steel slag. While these conditions have produced promising test results, they are not conducive to industrial-scale implementation due to their high cost and impracticality.

Table 1: Different carbonation conditions of some steel slag.

Reference	Temperature	Pressure of CO_2	Concentration of CO_2
[22]	100°C	1,000 kPa	100 vol%
[23]	50°C	1,000 kPa	100 vol%
[24]	650°C	2,000 kPa	100 vol%
[25]	90°C	3,000 kPa	100 vol%
[4]	95°C	/	30 ml/min

Table 1 illustrates the carbonation conditions for some steel slag studies.

In addition to the aforementioned challenges, carbonating steel slag requires a low-cost and readily available carbon source. Therefore, industrial exhaust gases containing CO_2 emerge as a favorable choice for carbonation of steel slag. Common industrial waste gases containing CO_2 include natural gas turbine flue gas (3%–4%), coal-fired boiler flue gas (12%–14%), and cement kiln tail gas (14%–33%) [26]. Among these, cement kiln tail flue gas offers the advantage of relatively high CO_2 concentration. However, variations in specific production processes can result in differences in concentration; for instance, Chen Yongbo used cement kiln tail gas with a CO_2 concentration of 22.2% [27], while Huang Lan's study utilized flue gas with a concentration of only 8%–10% [28]. Nevertheless, cement kiln tail exhaust gas remains a high-quality carbon source for steel slag carbonation. Nonetheless, as previously mentioned, the limited CO_2 concentration in cement kiln tail gas presents a challenge. Thus, improving the efficiency and extent of carbonation at lower CO_2 concentrations becomes a critical issue to address. Consequently, this study aims to simulate cement kiln tail exhaust gas under laboratory conditions and investigate the carbonation mechanism of steel slag within cementitious systems at lower CO_2 concentrations, providing a foundation for the further application of steel slag carbonation.

2. Materials and Methods

2.1. Steel Slag Used in the Study. The steel slag used in this study is layer-poured steel slag from Hebei, China, and its chemical composition is presented in Table 2. Steel slag comprises several primary chemical components, with a significant mass fraction, including 37.8% CaO, 29.2% Fe_2O_3, 11.6% SiO_2, 10.1% MgO, 5.9% Al_2O_3, 1.5% P_2O_5, 1.6% MnO, 0.8% TiO_2, and 0.2% Cr_2O_3. These components collectively constitute the chemical composition of steel slag, influencing its properties and applications. A high CaO content in steel slag is beneficial for its reactivity with CO_2. This is because CaO is highly reactive with CO_2 [29]. During carbonation, CaO in steel slag reacts with CO_2 from the environment to form $CaCO_3$, a stable and environmentally benign compound. This reaction helps sequester CO_2 from the atmosphere, making steel slag with a high CaO content an effective carbon capture and utilization material.

The X-ray diffraction (XRD) diagram of the steel slag is displayed in Figure 1. The primary mineral components of steel slag include C_2S, RO phases, $Ca_2Fe_2O_5$, and $Ca_{12}Al_{14}O_{33}$, and it also contains a small amount of C_3S and f-CaO.

Table 2: The chemical composition of steel slag.

	CaO	Fe_2O_3	SiO_2	MgO	Al_2O_3	P_2O_5	MnO	TiO_2	Cr_2O_3
Mass fraction *w*/%	37.8	29.2	11.6	10.1	5.9	1.5	1.6	0.8	0.2

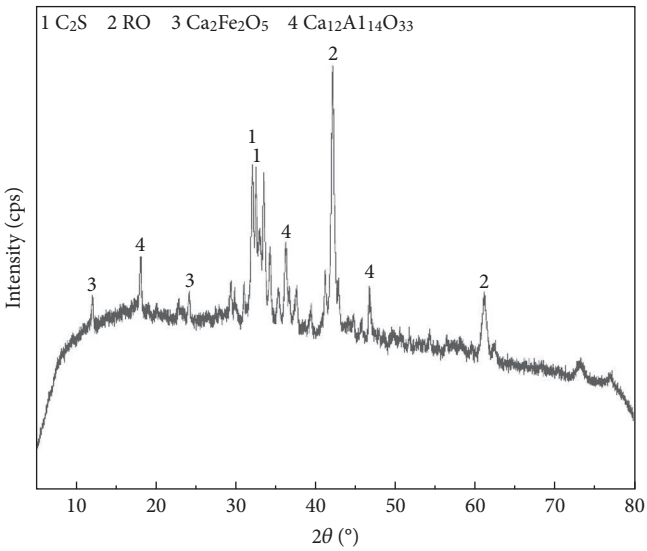

Figure 1: The XRD pattern of the steel slag.

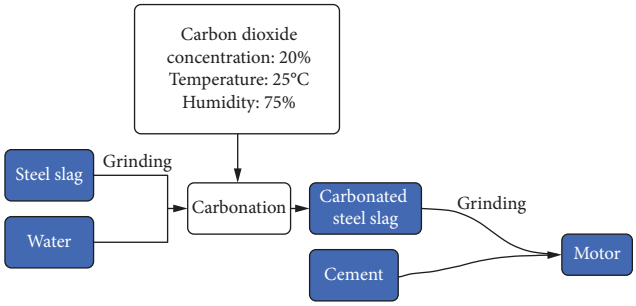

Figure 2: Basic process of preparing admixture.

In this study, the steel slag powder was ground to a particle size of less than 150 μm. The steel slag powder was carbonated by changing different carbonation conditions to explore the effects of carbonation conditions on the properties of the carbonated steel slag admixture.

2.2. Preparation and Test Methods of Carbonated Steel Slag. As shown in Figure 2, the basic process of preparing an admixture from steel slag powder is as follows: the steel slag powder is thoroughly mixed with a portion of the water and then placed into a shallow dish for carbonation. The carbonation atmosphere is provided by a concrete carbonation box that regulates temperature, humidity, and CO_2 concentration. After carbonation, the carbonated steel slag powder is ground to a particle size of less than 150 μm to obtain a carbonated steel slag admixture. For the sake of clarity, this study refers to the ratio of water and steel slag powder as the liquid–solid ratio. The carbonation conditions provided by the carbonation box are as follows: 20% CO_2 concentration, temperature at 25°C, and humidity at 75%.

The influence of different carbonation conditions on the performance of the carbonated steel slag admixture was explored. The fixed liquid–solid ratio is 20%, and the carbonation times are 12 hr, 1, 3, 7, and 14 days, respectively. The samples under these conditions are recorded as *T*1–*T*5. The fixed carbonation time is 3 days, and the liquid–solid ratios are 0%, 10%, 20%, 30%, 50%, and 100%, respectively. These samples are recorded as *W*0–*W*5.

In addition to the two influencing factors of carbonation time and liquid–solid ratio, this study also investigated the influence of alkali activators on the carbonation of steel slag powder. Alkali activators can effectively enhance the reactivity of steel slag. Therefore, in this study, NaOH and $Na_2SiO_3{\cdot}9H_2O$ were selected as alkali activators and added to the samples in an amount equal to 0.75% of the mass of steel slag powder to increase the carbonation rate. When NaOH was chosen as the alkali activator, the fixed liquid–solid ratio was 50%, and the carbonation times were 3 and 7 days. These two samples were recorded as *H*1 and *H*2, respectively. Subsequently, when $Na_2SiO_3{\cdot}9H_2O$ was used as the alkali activator, these two samples were recorded as *H*3 and *H*4.

Samples including *T*1–*T*5, *W*0–*W*5, and *H*1–*H*4 were subjected to thermogravimetric analysis (TGA), XRD, and content of f-CaO tests. XRD measurements were conducted from 5° to 90° (2θ) with a step size of 0.01°. TGA involved heating approximately 30 mg of powder in an alumina crucible at a uniform rate of 10°C/min from ambient temperature to 1,000°C, in a nitrogen flow of 50 ml/min. The f-CaO content was determined according to the standard of GB/T176-2017. For the carbonated steel slag tests mentioned above, XRD was used to investigate the phase changes before and after carbonation of steel slag, TGA was employed to study the carbon sequestration capacity of steel slag, and the f-CaO content was used to evaluate the volume stability of carbonated steel slag.

To further explore the performance of carbonated steel slag powder as an admixture, samples such as *T*1–*T*5, *W*0–*W*5, and *H*1–*H*4 were used to create mortar specimens, and their compressive/flexural strengths were tested to assess the mechanical properties of carbonated steel slag. The specific test method involved replacing P·I 42.5 cement with the admixture in a proportion of 30%, preparing the mortar according to the standard of GB/T17671-1999, and conducting compressive and flexural strength tests at 7 and 28 days. Steel slag without carbonation was also tested as a blank sample.

In addition, all samples were mixed at a ratio of 30% carbonated steel slag powder and 70% cement, with a liquid–solid ratio of 0.5, to create paste samples. These paste samples were then subjected to XRD, scanning electron microscopy—backscattered electron (SEM-BSE), and mercury intrusion porosimetry (MIP) tests to explore the effect of carbonated steel slag on the phase changes and microstructure of the cementitious system.

Table 3: Different carbonation conditions of all samples.

Number of sample	Carbonation time	Liquid–solid ratio	Alkali activator
*T*1	12 hr	20%	–
*T*2	1 days	20%	–
*T*3	3 days	20%	–
*T*4	7 days	20%	–
*T*5	14 days	20%	–
*W*0	3 days	0%	–
*W*1	3 days	10%	–
*W*2	3 days	20%	–
*W*3	3 days	30%	–
*W*4	3 days	50%	–
*W*5	3 days	100%	–
*H*1	3 days	50%	NaOH
*H*2	7 days	50%	NaOH
*H*3	3 days	50%	$Na_2SiO_3{\cdot}9H_2O$
*H*4	7 days	50%	$Na_2SiO_3{\cdot}9H_2O$

Specific changes in carbonation conditions can also be found in Table 3.

2.3. Method of Evaluating Carbonation Efficiency of Steel Slag. Currently, the evaluation of steel slag's carbonation efficiency varies depending on its intended use as carbonated steel slag. In this study, CO_2 uptake and carbonation degree, determined through the mass loss method, were employed to assess the carbonation efficiency based on TGA [30]. The calculation of CO_2 uptake and carbonation degree is presented in Equations (1)–(4).

$$CO_2\text{uptake}, 100\% = \frac{\text{Mass of reacted } CO_2}{\text{Mass of } CO_2 \text{ reactants}} \times 100\%, \tag{1}$$

$$CO_2\text{uptake}, 100\% = \frac{(\text{Mass at } 550\,^{\circ}\text{C} - \text{Mass at } 1{,}000\,^{\circ}\text{C})}{\text{Mass of } CO_2 \text{ reactants}} \times 100\%, \tag{2}$$

$$\text{Carbonation degree}, 100\% = \frac{CO_2 \text{ Uptake}}{\text{Maximum } CO_2 \text{ uptake}} \times 100\%, \tag{3}$$

$$\text{Maximum } CO_2 \text{ uptake}, 100\% = 0.785\,(CaO \times 0.56\,CaCO_3 \times 0.7\,SO_3) + 1.01\,MgO + 1.42\,Na_2O + 0.93\,K_2O. \tag{4}$$

3. Results and Discussion

3.1. Properties of Carbonated Steel Slag

3.1.1. Phase Change of Carbonated Steel Slag. Figure 3 presents the XRD patterns of steel slag powder with varying carbonation times. As observed in the figure, the diffraction peaks of the original C_2S and RO phases in the steel slag decrease significantly during the carbonation reaction. In addition, it can be noted that the diffraction peak of $CaCO_3$ (Calcite) is rising, indicating continuous conversion of the carbonable phase in the steel slag to $CaCO_3$. Notably, when compared to the blank sample, the $CaCO_3$ diffraction peak in *T*1–*T*5 is quite distinct, signifying substantial $CaCO_3$ formation. For samples *T*1–*T*5, it is evident that as the carbonation time increases, the diffraction peaks of C_2S and RO gradually weaken, while the $CaCO_3$ diffraction peak gradually strengthens, suggesting an increasing $CaCO_3$ content in the samples. No diffraction peak of $Ca(OH)_2$ was observed in the XRD patterns, as $Ca(OH)_2$ produced by C_2S hydration was converted to $CaCO_3$. The carbonation reaction

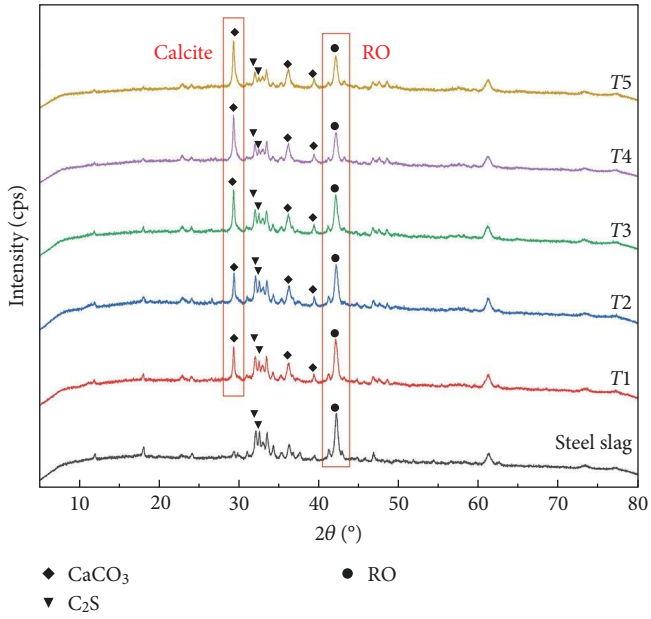

Figure 3: XRD patterns of steel slag with different carbonation time.

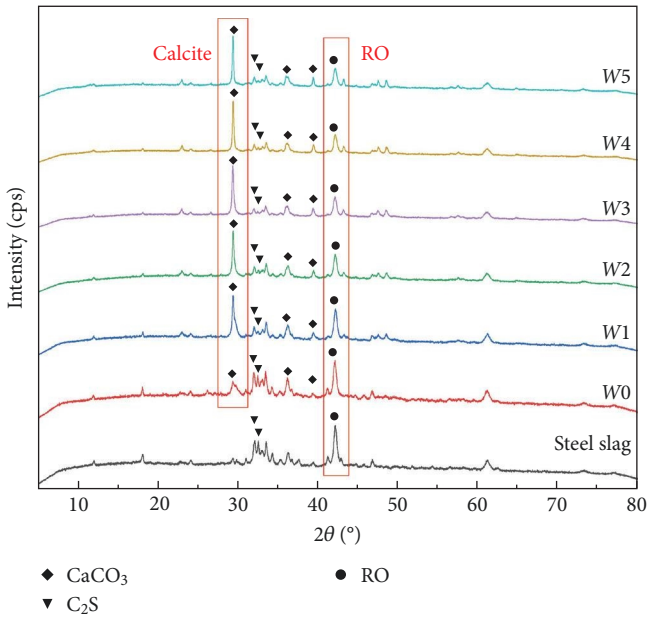

Figure 4: XRD patterns of steel slag with different liquid–solid ration.

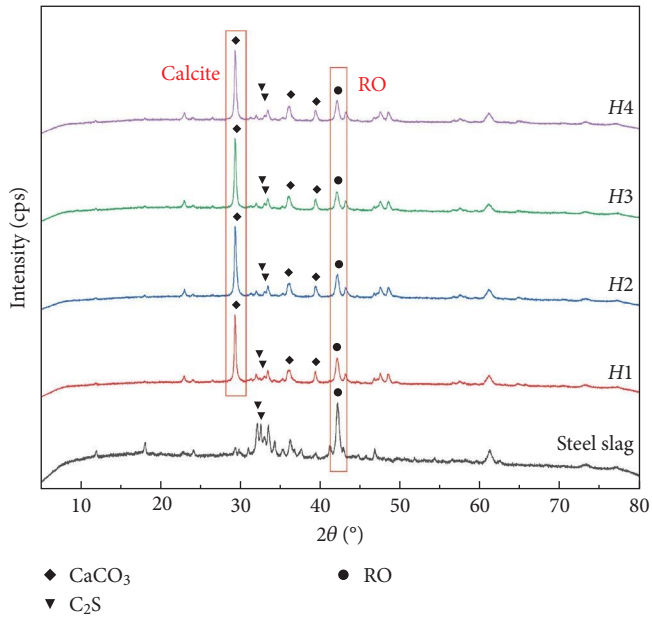

Figure 5: XRD patterns of steel slag with alkali activator.

continues to progress over a certain carbonation time, and extending this time benefits the enhancement of the carbonation degree.

The XRD results of *W*0–*W*5 are depicted in Figure 4. The patterns of *W*0–*W*5 demonstrate that altering the liquid–solid ratio primarily affects the carbonation degree, with no generation of new phases. With the gradual increase in the liquid–solid ratio, the diffraction peak of $CaCO_3$ exhibits an initial increase, reaching its maximum at a liquid–solid ratio of 50%, after which it starts to decline. Consequently, the highest carbonation efficiency is achieved at a liquid–solid ratio of 50%.

The XRD results of *H*1–*H*4 are illustrated in Figure 5. Similar to the effect of the liquid–solid ratio, the addition of the alkali activator does not result in the generation of new phases during carbonation. However, it effectively enhances the carbonation efficiency, with a prominent $CaCO_3$ peak.

In conclusion, the XRD results can be summarized as follows: first, prolonging the carbonation time effectively enhances the degree of carbonation. Second, for carbonating steel slag powder, the highest efficiency is achieved with a liquid–solid ratio of 50%, corresponding to the highest degree of carbonation at the same age. Furthermore, after carbonating all the samples, there is a significant reduction in RO phases, including f-CaO, which effectively enhances the stability of steel slag.

The XRD results clearly indicate that the primary product of steel slag carbonation is $CaCO_3$, specifically in the form of calcite. To further confirm the crystal form of $CaCO_3$, scanning electron microscopy—energy dispersive X-ray spectroscopy (SEM-EDS) testing was conducted on the carbonated steel slag. Figure 6 and Table 4 displays the typical microscopic morphology of carbonated steel slag powder, with certain $CaCO_3$ grains marked. By combining the XRD results with the microscopic morphology observed through SEM-EDS, it can be confidently stated that the $CaCO_3$ formed after steel slag carbonation is indeed calcite. Calcite exhibits a small grain size, measuring only about 1 μm in diameter.

When these fine calcite particles are introduced into the cementitious system, they serve two crucial functions. First, they facilitate the nucleation of hydration products. Second, both the calcite particles themselves and the hydration products formed in their vicinity effectively fill the voids within the cementitious system, thereby enhancing its overall density.

3.1.2. Carbonation Efficiency and Stability of Carbonated Steel Slag. CO_2 uptake and carbonation degree/content of f-CaO for carbonated steel slag powder are shown in Figures 7–9.

The test data reveals that the CO_2 uptake of carbonated steel slag powder falls within the range of 5.0%–20.1%, and the carbonation degree ranges from 12.3% to 49.4% (with the theoretical maximum CO_2 uptake being 40.6%). This implies that every 1 ton of steel slag powder can capture between 50 and 201 kg of CO_2 (calculated based on the CO_2 uptake of the samples).

As depicted in Figure 7, both the CO_2 uptake and carbonation degree of the samples continue to increase as the carbonation time progresses. However, as the carbonation time extends, the rate of increase in CO_2 uptake and carbonation degree gradually slows down. While extending the carbonation time is beneficial for enhancing carbonation efficiency, the improvement in carbonation becomes progressively limited during longer carbonation periods. Furthermore, as the carbonation reaction proceeds, the content of f-CaO in the samples steadily decreases. This phenomenon indicates that f-CaO is partially or even completely consumed as a result of the carbonation reaction, effectively enhancing the stability of steel slag.

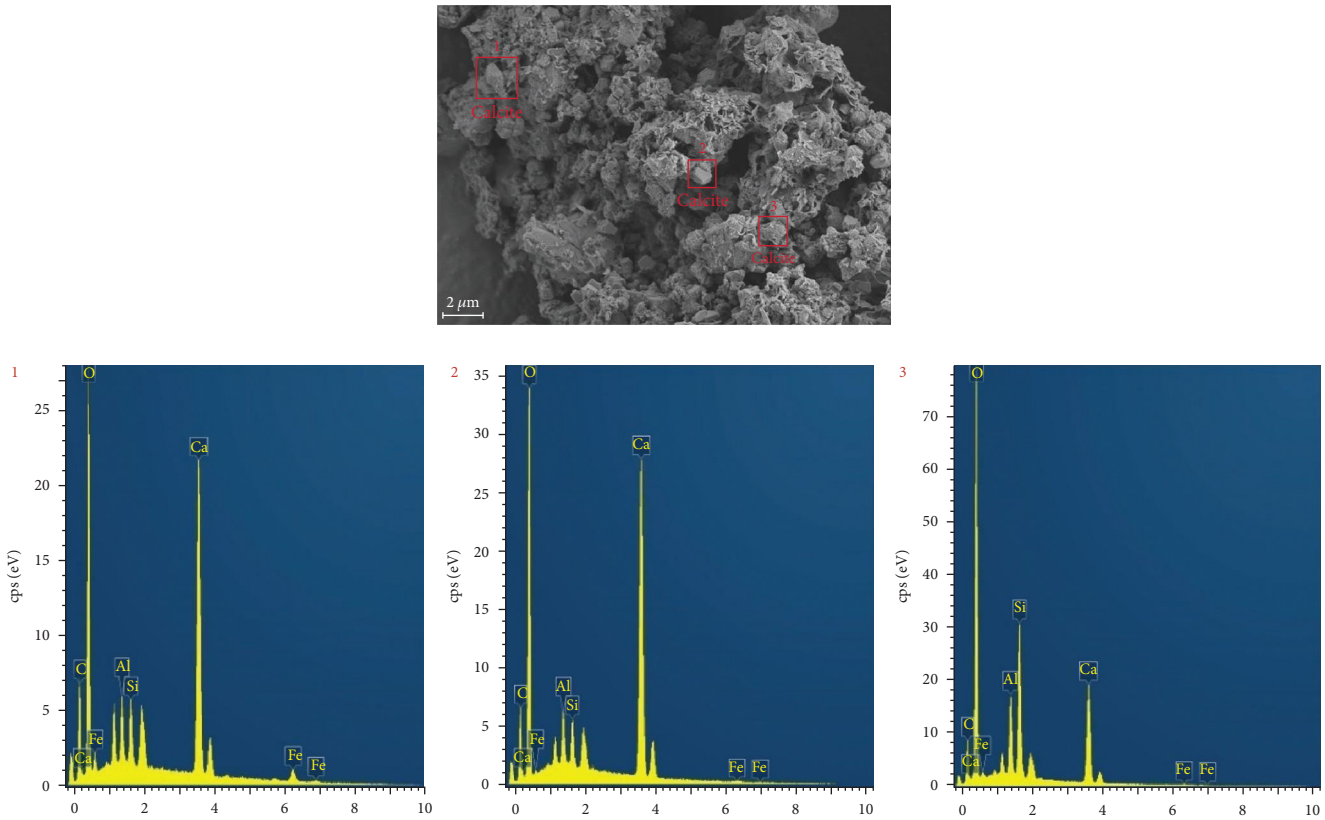

Figure 6: SEM-EDS picture of *W*4.

Table 4: EDS spectroscopy results of *W*4 samples (corresponding to Figure 6).

	C (%)	O (%)	Al (%)	Si (%)	Ca (%)	Fe (%)
1	18.48	49.14	2.04	2.08	23.13	5.14
2	13.34	57.45	1.72	1.62	25.60	0.27
3	15.64	61.01	3.72	7.68	11.38	0.57

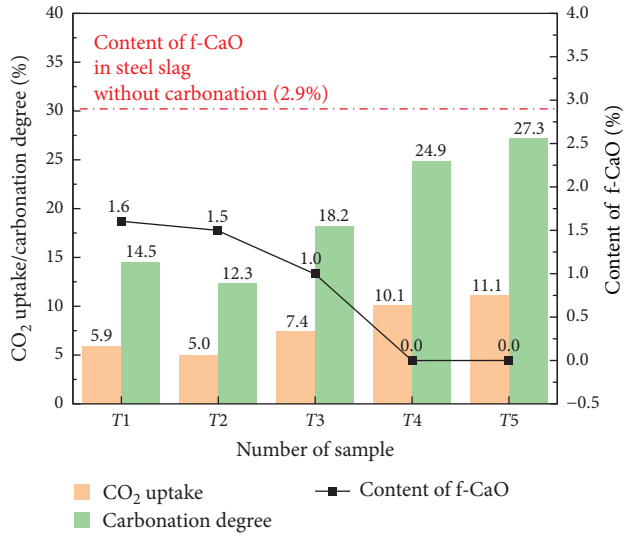

Figure 7: CO_2 uptake and carbonation degree/content of f-CaO of *T*1–*T*5.

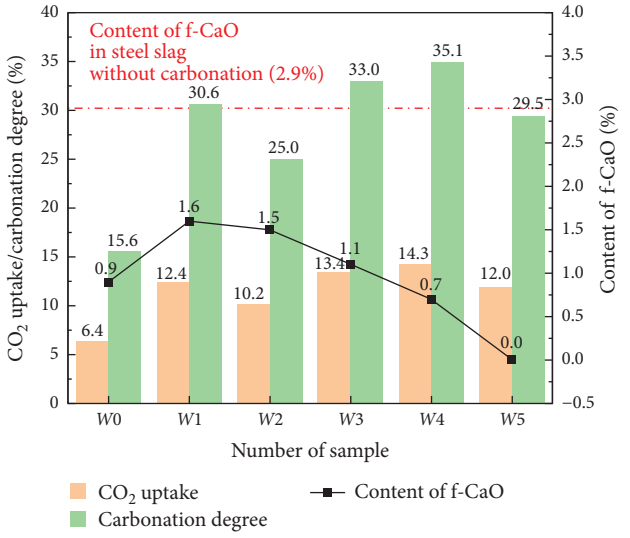

Figure 8: CO_2 uptake and carbonation degree/content of f-CaO of *W*0–*W*5.

As demonstrated in Figure 8, the liquid–solid ratio significantly impacts both the CO_2 uptake and carbonation degree. With a continuous increase in the liquid–solid ratio, there is a noticeable trend of initially increasing and then decreasing CO_2 uptake and carbonation degree. The maximum values are reached when the liquid–solid ratio is 50%, after which they start to decline. This phenomenon is primarily

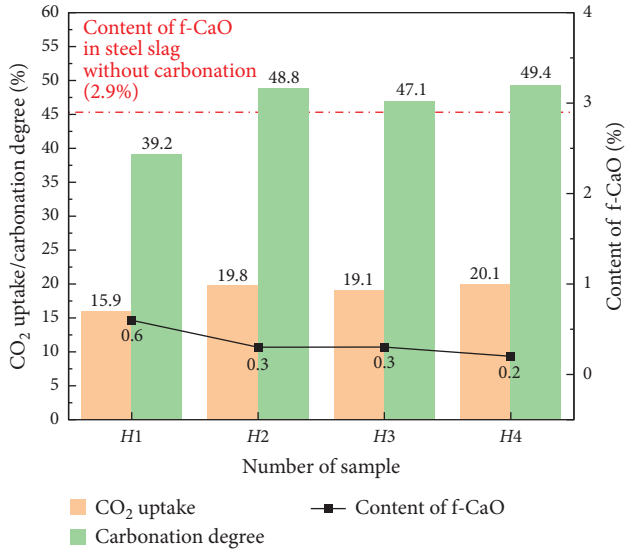

Figure 9: CO_2 uptake and carbonation degree/content of f-CaO of *H*1–*H*4.

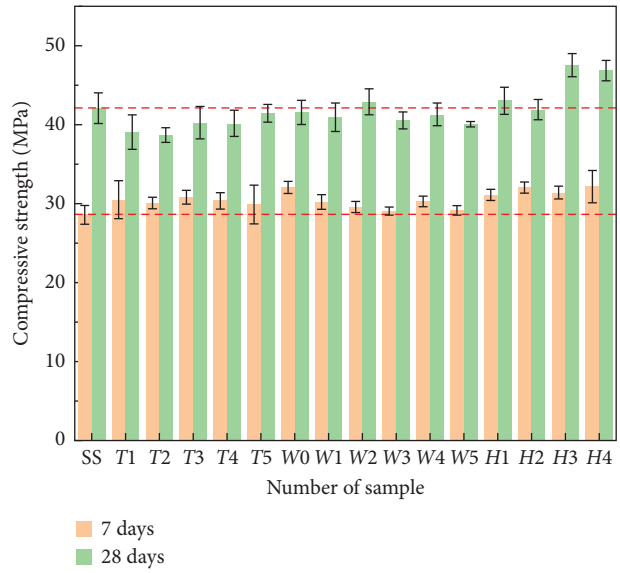

Figure 10: Compressive strength of all samples at 7 and 28 days.

due to the carbonation process of steel slag, which necessitates the presence of both water and CO_2 [31]. When the liquid–solid ratio is low, water is consumed as the reaction progresses, making it challenging for the carbonation reaction to occur, resulting in lower carbonation efficiency. Conversely, when the liquid–solid ratio is high, it leads to the steel slag particles being surrounded by water, making it difficult for CO_2 to contact the steel slag particles, again resulting in lower carbonation efficiency. Notably, the content of f-CaO in samples with a liquid-to-solid ratio of 100% is the lowest, at 0%. The overall trend is an initial increase followed by a decrease. In contrast to *T*1–*T*5, the main influencing factor for the f-CaO content of samples *W*0–*W*5 is the liquid–solid ratio, not the CO_2 uptake. Compared with *W*0 and *W*1–*W*5, the *W*0 samples had lower CO_2 uptake but higher f-CaO content. However, *W*0 samples remain in powdered form after carbonation, while *W*1–*W*5 samples agglomerate. In industrial applications, *W*1–*W*5 samples require additional energy for secondary grinding, making the carbonation conditions of *W*0 more suitable for industrial production.

As illustrated in Figure 9, the alkali activator also exerts a significant influence on the rate of the carbonation reaction. The addition of NaOH and $Na_2SiO_3{\cdot}9H_2O$ has led to a notable improvement in both CO_2 uptake and carbonation degree. Specifically, samples with $Na_2SiO_3{\cdot}9H_2O$ added at 3 and 7 days exhibited significant improvements compared to samples without an alkali activator. Samples with NaOH added showed a substantial improvement at 7 days. In the case of *H*1–*H*4, the f-CaO content decreased compared to *W*4. Nevertheless, the f-CaO content of *H*1–*H*4 remains higher than that of *W*5, reaffirming that the primary factor affecting f-CaO content is the liquid–solid ratio.

In conclusion, to enhance CO_2 uptake, extending the carbonation time should be considered as the first step, with CO_2 uptake increasing from 5.9% at 12 hr to 11.1% at 14 days. Second, selecting the appropriate liquid–solid ratio is crucial. The study's experimental results indicate that a liquid–solid ratio of 50% results in the highest carbonation efficiency, with CO_2 uptake reaching 14.3% at 3 days. In addition, an alkali activator can effectively improve carbonation efficiency, particularly $Na_2SiO_3{\cdot}9H_2O$, where CO_2 uptake can reach 20.1% at 7 days.

Regarding the influencing factors on f-CaO content, the most significant factor is the liquid–solid ratio used during the carbonation treatment in this study. When the liquid–solid ratio is 100%, all f-CaO can be consumed within 3 days. Furthermore, under constant liquid–solid ratio conditions, increasing CO_2 uptake can also lead to greater f-CaO consumption.

3.2. Carbonated Steel Slag as Admixtures in Cementitious System

3.2.1. Mechanical Properties. The influence of carbonated steel slag as a mineral admixture is reflected in the compressive and flexural strength of the mortar, and the test results are presented in Figures 10 and 11 and Table 5.

The addition of carbonated steel slag powder leads to a slight improvement in the compressive strength and flexural strength of the mortar at 7 days, but there is no significant improvement at 28 days. However, the flexural strength does show improvement at both 7 and 28 days. As indicated by *T*1–*T*5, with the extension of carbonation time and the increase in carbonation degree, the compressive and flexural strength do not exhibit significant increases, and the changes are minimal. It is noteworthy that the 28-day flexural strength of the mortar specimen made with *W*5 suggests that an excessively long carbonation time for steel slag powder may have a detrimental effect on the flexural strength of the cementitious system.

A similar trend can be observed in *W*0–*W*5, even though the overall carbonation degree of the *W*0–*W*5 samples is relatively higher compared to *T*1–*T*5. However, there is no

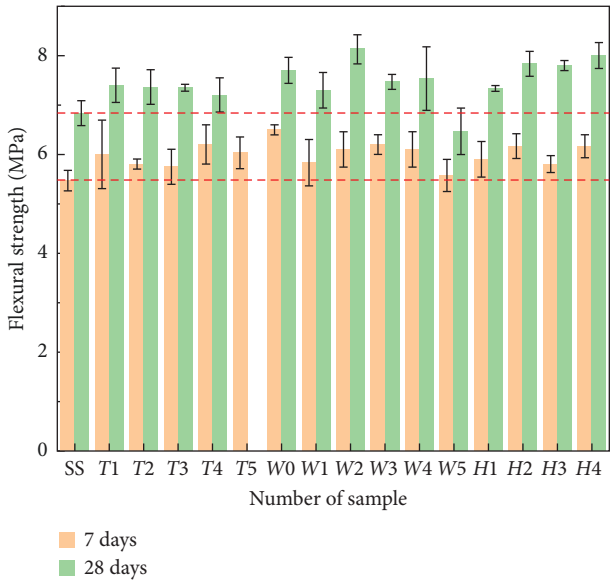

Figure 11: Flexural strength of all samples at 7 and 28 days.

Table 5: The compressive and flexural strength of steel slag.

Number of sample	Compressive strength (MPa)		Flexural strength (MPa)	
	7 days	28 days	7 days	28 days
Blank sample	28.6	42.1	5.5	6.8
*T*1	30.5	39.1	6.0	7.4
*T*2	30.1	38.7	5.8	7.4
*T*3	30.8	40.3	5.8	7.3
*T*4	30.4	40.2	6.2	7.2
*T*5	29.9	41.5	6.0	0
*W*0	32.1	41.5	6.5	7.7
*W*1	30.2	40.9	5.8	7.3
*W*2	29.6	42.9	6.1	8.1
*W*3	29.0	40.5	6.2	7.5
*W*4	30.3	41.3	6.1	7.5
*W*5	29.1	40.0	5.6	6.5
*H*1	31.1	43.0	5.9	7.3
*H*2	32.0	41.9	6.2	7.8
*H*3	31.4	47.5	5.8	7.8
*H*4	32.2	46.9	6.2	8.0

significant improvement in the compressive and flexural strength, despite the increase in carbonation degree.

The results for *H*1–*H*4 show that the compressive and flexural strength of the NaOH samples align with the trends observed in the previous two groups of samples, with only slight improvements. However, when the sample was carbonated with $Na_2SiO_3{\cdot}9H_2O$, its compressive strength exhibited significant improvement compared to the blank steel slag, with an increase of approximately 3.0–4.0 MPa at 7 days and 5.0 MPa at 28 days.

The increase in compressive and flexural strength is primarily attributed to the presence of a certain amount of

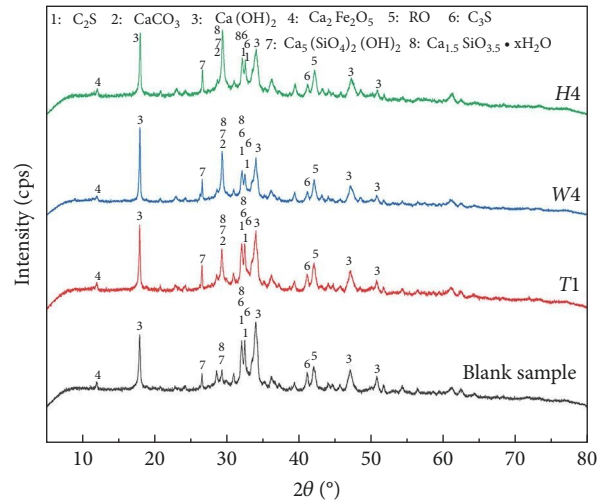

Figure 12: The XRD pattern of paste samples of blank sample, *T*1, *W*4, and *H*4 in 7 days.

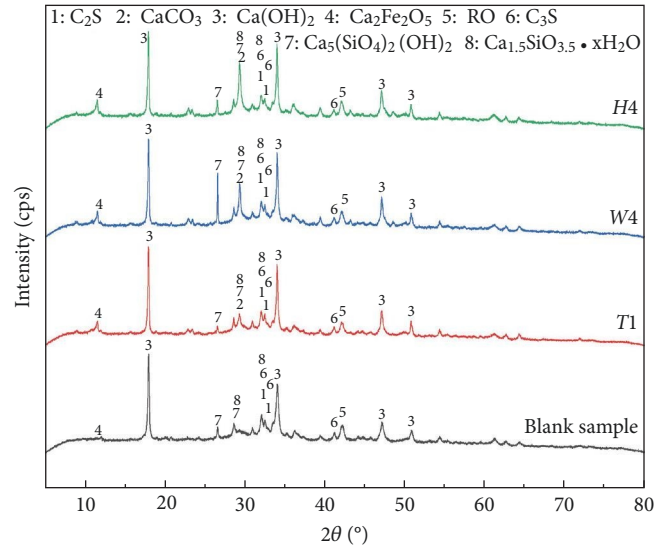

Figure 13: The XRD pattern of paste samples of blank sample, *T*1, *W*4, and *H*4 in 28 days.

$CaCO_3$ seeds in the carbonated steel slag powder. The addition of these $CaCO_3$ seeds accelerates the formation of hydration products, thereby enhancing both compressive and flexural strength, especially in the early stages [32]. It is evident that the compressive and flexural strength of all carbonated samples at 7 days exhibits improvement compared to the blank sample [33].

To sum up, the addition of carbonated steel slag powder can improve the mechanical properties of the cementitious system. When the carbonated steel slag powder content is 30%, the flexural strength can increase by about 0.5 MPa in 7 days and increase by about 0.5–1.0 MPa in 28 days. The compressive strength can increase by 2.0–3.0 MPa in 7 days, and compressive strength has no significant increase in 28 days. In addition, it should be noted that the carbonation

Table 6: The porosity and median pore diameter (volume) of blank sample and *W*4.

Number of sample	Age (days)	Porosity (%)	Median pore diameter (volume) (nm)
Blank sample	7	38.1	72.8
*W*4	7	36.7	52.1
Blank sample	28	35.9	42.0
*W*4	28	37.7	35.6

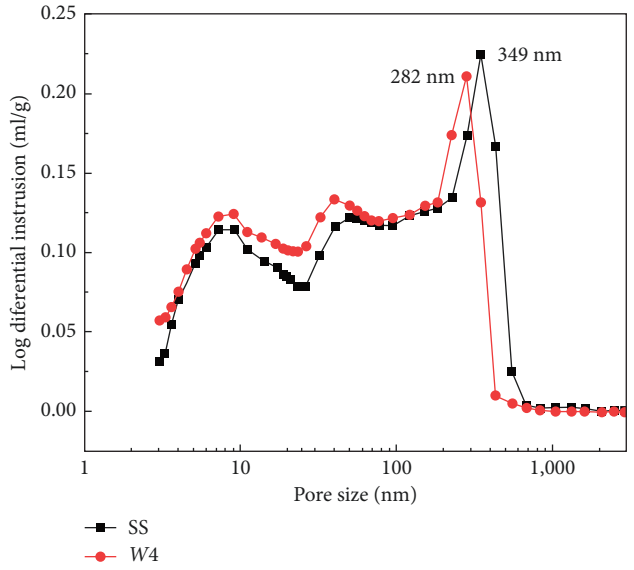

Figure 14: Pore structure distribution of blank sample and *W*4 in 7 days.

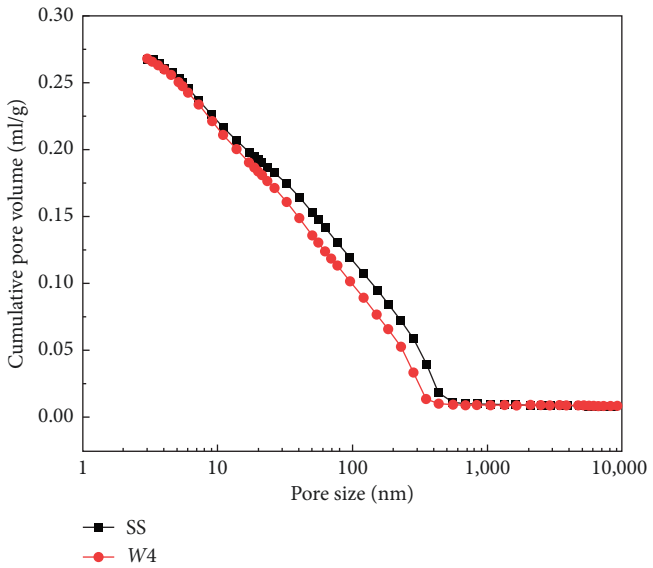

Figure 15: Cumulative porosity of blank sample and *W*4 in 7 days.

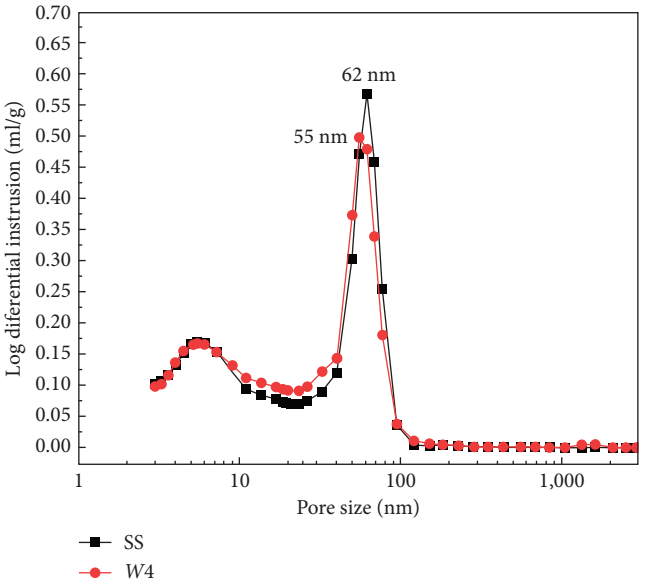

Figure 16: Pore structure distribution of blank sample and *W*4 in 28 days.

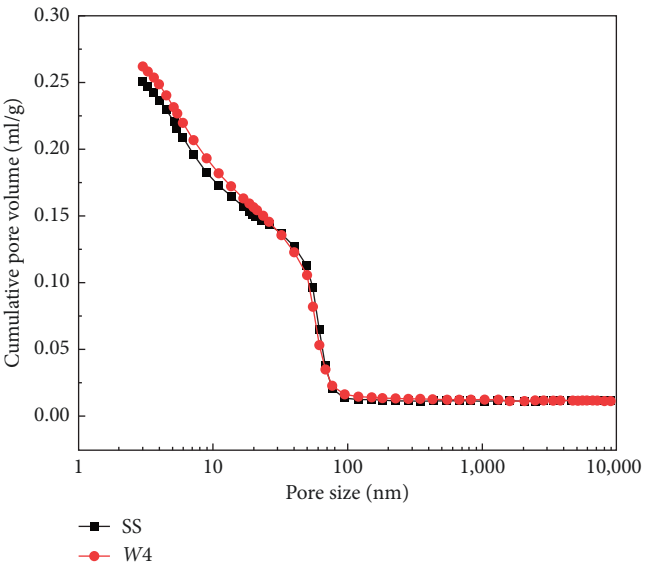

Figure 17: Cumulative porosity of blank sample and *W*4 in 28 days.

time of carbonated steel slag powder should not be too long, and the flexural strength of *W*5 is 0. Moreover, the mechanical properties of the samples added with $Na_2SiO_3{\cdot}9H_2O$ during carbonation are better than NaOH, and the compressive strength is improved obviously both in 7 and 28 days.

3.2.2. Impact of Carbonated Steel Slag on the Cementitious System. XRD results for some representative paste samples are shown in Figures 12 and 13.

It can be seen from the figure that the main phases in the hydrated paste sample are C_2S, $CaCO_3$, $Ca(OH)_2$, $Ca_2Fe_2O_5$,

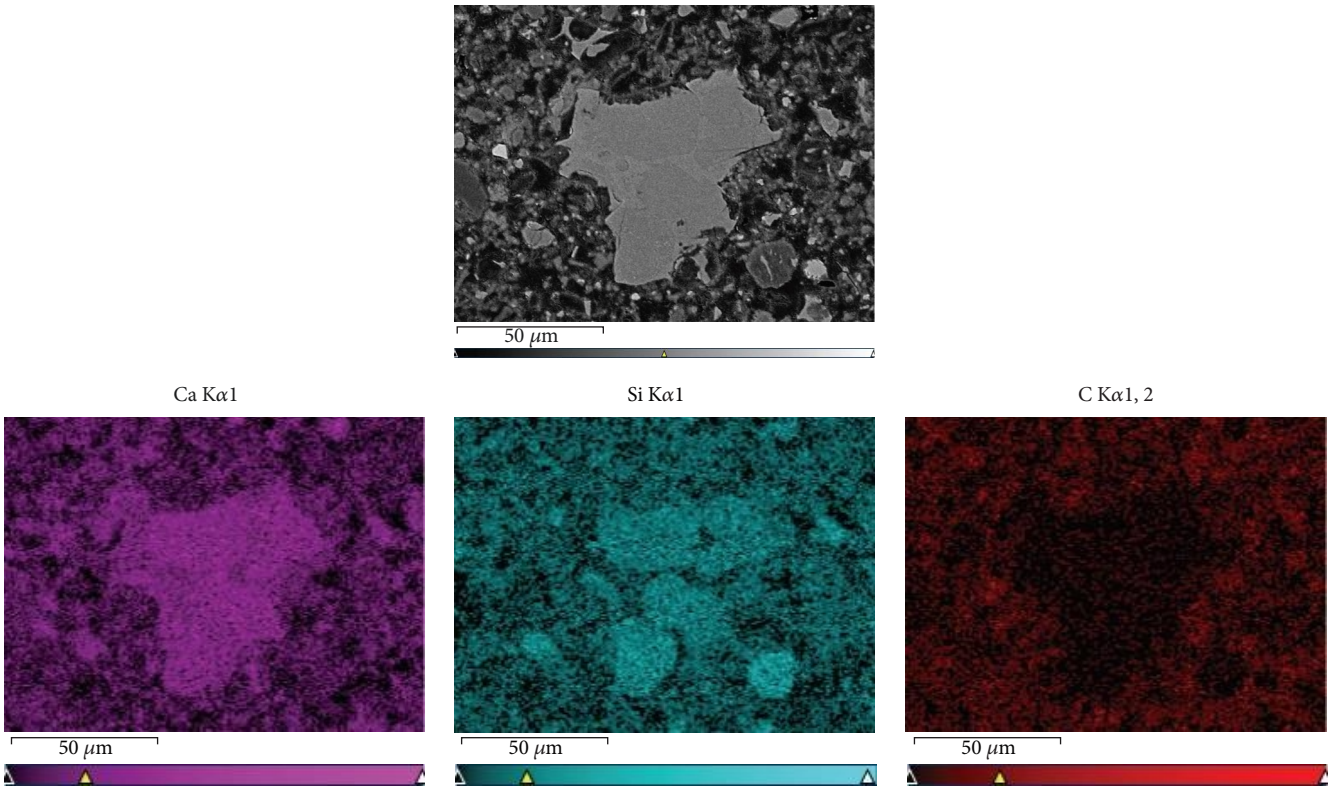

Figure 18: SEM-BSE picture of W4 and element distribution of Ca, Si, and C (3 days).

RO phase, C_3S, $Ca_5(SiO_4)_2(OH)_2$, and $Ca_{1.5}SiO_{3.5}{\cdot}xH_2O$. These phases can also be mainly divided into two categories, one is from the cement and carbonated steel slag itself including C_3S, C_2S, RO phase, $Ca_2Fe_2O_5$, and $CaCO_3$, and the other is the hydration products of cement and carbonated steel slag including $Ca_5(SiO_4)_2(OH)_2$, $Ca_{1.5}SiO_{3.5}{\cdot}xH_2O$, and $Ca(OH)_2$. At the same time, it can also be seen that the sample added to the carbonated steel slag powder has a higher amount of hydration products at the same age, especially the C–S–H phase such as $Ca_5(SiO_4)_2(OH)_2$ and $Ca_{1.5}SiO_{3.5}{\cdot}xH_2O$. The increase of hydration products should be the influence of $CaCO_3$ grains, which help the nucleation of hydration products and accelerate hydration to a certain extent.

The results of MIP are presented in Table 6 and Figures 14–17. First, it can be observed from Table 6 that there is not much difference in porosity between the blank sample and the *W*4 sample. However, the *W*4 sample containing carbonated steel slag powder exhibited a median pore diameter (volume) of 52.1 nm at 7 days, whereas the blank sample had a median pore diameter (volume) of 72.8 nm at 7 days. At 28 days, the *W*4 sample displayed a median pore diameter (volume) of 35.6 nm, while the blank sample had a median pore diameter (volume) of 42.0 nm at 28 days.

As evident from Figures 15 to 17, the cumulative porosity of the *W*4 sample and the blank sample does not show significant differences. However, as seen in Figures 14–16, the pore size in the sample containing carbonated steel slag powder is considerably reduced and finer. At 7 days, the pores in the *W*4 sample were concentrated around 282 nm, whereas the pores in the blank sample were concentrated at a much higher value, around 349 nm. At 28 days, the pores in the *W*4 sample were concentrated around 55 nm, while the pores in the blank sample were concentrated around 62 nm.

Based on the MIP results, it can be concluded that the addition of carbonated steel slag powder effectively reduces the pore diameter within the cementitious system, mitigating potential issues associated with larger pores. This is attributed to the role played by carbonated steel slag powder in nucleating and filling pores. Coupled with the previous findings on mechanical properties, all the mortar samples mentioned above displayed enhanced compressive and flexural strength at 7 days, likely due to the improved pore structure during this period. However, as the age reached 28 days, carbonated steel slag no longer contributes significantly to nucleation during the later stages of cementitious system hydration. At this point, hydration product formation is relatively dense, resulting in less reduction in median pore diameter (volume) at 28 days compared to the improvement observed at 7 days [34].

Figure 18 displays SEM-BSE photographs and elemental distribution maps of *W*4 samples (3 days). When examining the photograph and the elemental distribution map, it becomes apparent that the largest light-colored area in the photo represents the Ca–Si phase, while other small particles and pores are distributed around the Ca–Si phase. Notably, the distribution of the C element is primarily concentrated in the regions containing small particles and pores. In conjunction with the preceding information, it can be inferred that the $CaCO_3$ grains generated during carbonation are primarily distributed in these areas.

The results obtained from SEM-BSE corroborate the earlier conclusion that the addition of $CaCO_3$ grains contributes to nucleation, pore filling, pore diameter reduction within the cementitious system, overall density improvement, and enhancement of mechanical properties.

4. Conclusions

In this study, the impact of low CO_2 concentration on carbonated steel slag admixtures was investigated by subjecting steel slag powder to carbonation under various conditions. In addition, carbonated steel slag powder was incorporated into mortar and paste samples to assess its influence on the hydration and microstructure of the cementitious system. The following key conclusions have been derived:

(1) The primary product of steel slag carbonation is $CaCO_3$, predominantly in the form of calcite, characterized by its small particle size, averaging around 1 μm. The introduction of these $CaCO_3$ particles alongside carbonated steel slag into the cementitious system facilitates nucleation and pore-filling, resulting in reduced pore diameter within the paste. This enhancement leads to improved compactness and strength.

(2) Several factors, including carbonation time, liquid–solid ratio, and the addition of alkali activators, impact the CO_2 uptake of carbonated steel slag powder. Longer carbonation times and the use of alkali activators positively affect CO_2 uptake. Remarkably, a liquid–solid ratio of 50% yields higher CO_2 uptake. Among the alkali activators tested, $Na_2SiO_3{\cdot}9H_2O$ proves more effective, achieving a CO_2 uptake of up to 16.0%.

(3) Carbonation leads to the conversion of f-CaO in steel slag to $CaCO_3$, enhancing stability. The most significant factor affecting f-CaO content is the liquid–solid ratio employed during carbonation. A ratio of 50% reduces f-CaO content to 0% in 7 days. However, at a ratio of 20%, it is reduced to only 1.5% in the same timeframe. Furthermore, under consistent liquid–solid ratios, increasing carbonation time and incorporating alkali activators can further reduce f-CaO content.

(4) Incorporating carbonated steel slag powder generally enhances the mechanical properties of the cementitious system. Compressive strength increases at 7 days, and flexural strength improves at both 7 and 28 days. It is essential to note that excessive carbonation time negatively impacts flexural strength. The 14-day carbonation time of the *T*5 sample resulted in complete loss of flexural strength.

(5) Considering comprehensive factors such as carbon sequestration capacity, stability, and mechanical properties, the study recommends a carbonation time of 3–7 days, a liquid–solid ratio of 50%, and the utilization of $Na_2SiO_3{\cdot}9H_2O$ as an alkali activator for steel slag powder carbonation.

Data Availability

Data available on request. If you need relevant data for research, you can contact Mr. Sun.

Conflicts of Interest

The authors declare that they have no conflicts of interest.

Acknowledgments

This work was supported by the Beijing Science and Technology Planning Project (Z221100007522002).

References

[1] A. Omar and K. Muthusamy, "Concrete industry, environment issue, and green concrete: a review," *Construction*, vol. 2, no. 1, pp. 1–9, 2022.

[2] A. Raza, R. Gholami, R. Rezaee, V. Rasouli, and M. Rabiei, "Significant aspects of carbon capture and storage—a review," *Petroleum*, vol. 5, no. 4, pp. 335–340, 2019.

[3] M. I. Jianfeng and M. A. Xiaofang, "Development trend analysis of carbon capture," *Utilization and Storage Technology in China*, vol. 39, no. 9, pp. 2537–2544, 2019.

[4] S. Yadav and A. Mehra, "Experimental study of dissolution of minerals and CO_2 sequestration in steel slag," *Waste Management*, vol. 64, pp. 348–357, 2017.

[5] W. A. N. G. Dongxing and H. E. Fujin, "Investigation on performance and mechanism of CO_2 carbonated slag/fly ash solidified soils," *Chinese Journal of Rock Mechanics and Engineering*, vol. 39, no. 7, pp. 1493–1502, 2020.

[6] G. Montes-Hernandez, R. Pérez-López, F. Renard, J. M. Nieto, and L. Charlet, "Mineral sequestration of CO_2 by aqueous carbonation of coal combustion fly-ash," *Journal of Hazardous Materials*, vol. 161, no. 2-3, pp. 1347–1354, 2009.

[7] L. I. Xinchuang and L. I. Bing, "Low carbon transition path of China's iron and steel industry under global temperature control target," *Iron and Steel*, vol. 54, no. 8, pp. 224–231, 2019.

[8] J. Guo, Y. Bao, and M. Wang, "Steel slag in China: treatment, recycling, and management," *Waste Management*, vol. 78, pp. 318–330, 2018.

[9] M. R. Hainin, M. M. A. Aziz, Z. Ali, R. Putra Jaya, M. M. El-Sergany, and H. Yaacob, "Steel slag as a road construction material," *Jurnal Teknologi*, vol. 73, no. 4, pp. 33–38, 2015.

[10] A. A. G. NadiatulAdilah, S. Y. AymanMohammed, P. J. Ramadhansyah, O. Rokiah, and M. R. Hainin, "The influence of steel slag as alternative aggregate in permeable concrete pavement," *IOP Conference Series: Materials Science and Engineering*, vol. 712, Article ID 012011, 2020.

[11] C. Zhimin, L. Rui, Z. Xianming, and L. Jiaxiang, "Carbon sequestration of steel slag and carbonation for activating RO phase," *Cement and Concrete Research*, vol. 139, 2021.

[12] R. M. Andrew, "Global CO_2 emissions from cement production, 1928–2018," *Earth System Science Data*, vol. 11, no. 4, pp. 1675–1710, 2019.

[13] Y. Jiang, T.-C. Ling, C. Shi, and S.-Y. Pan, "Characteristics of steel slags and their use in cement and concrete—a review," *Resources, Conservation and Recycling*, vol. 136, pp. 187–197, 2018.

[14] J. I. A. N. G. Ao, "Application and research of hydration mechanism of steel slag and its active excitation," *China Water Transport*, vol. 22, no. 2, pp. 159-160, 2022.

[15] W.-J. Tang, H.-Q. Liao, Y. Zhou, W.-J. Zhao, and H.-H. Chen, "Distribution of free-calcium oxide in converter slags and its stabilization," *Steelmaking*, vol. 25, no. 3, pp. 34–36, 2009.

[16] S.-W. Lee, Y.-J. Kim, Y.-H. Lee, H. Guim, and S. M. Han, "Behavior and characteristics of amorphous calcium carbonate and calcite using $CaCO_3$ film synthesis," *Materials & Design*, vol. 112, pp. 367–373, 2016.

[17] C. Shi, D. Wang, F. He, and M. Liu, "Weathering properties of CO_2-cured concrete blocks," *Resources, Conservation and Recycling*, vol. 65, pp. 11–17, 2012.

[18] Z. Duo and Y. Shao, "Surface scaling of CO_2-cured concrete exposed to freeze-thaw cycles," *Journal of CO_2 Utilization*, vol. 27, pp. 137–144, 2018.

[19] N. Luan, M. Yin, K. Chen, H.-T. Zhang, and Y.-C. Zhu, "The carbonation of steel slag and its influence on the properties of cement mortar," China Nonferrous Metallurgy, 2022.

[20] J. Song, *Carbonation Curing Solid Waste Non-burning Brick Formula Optimization Research and Industrial Demonstration*, Zhejiang University, 2021.

[21] Y. Chunyang, *Preparation of Carbonated Steel Slag Aggregates and Planting Concretes*, Dalian University of Technology, 2019.

[22] B. Renato, E. D. B. Giulia, A. Polettini, and R. Pomi, *Wet Versus Slurry Carbonation of EAF Steel Slag*, Greenhouse Gases Science & Technology, 2011.

[23] R. Baciocchi, G. Costa, E. Di Bartolomeo, A. Polettini, and R. Pomi, "Carbonation of stainless steel slag as a process for CO_2 storage and slag valorization," *Waste and Biomass Valorization*, vol. 1, no. 4, pp. 467–477, 2010.

[24] R. M. Santos, D. Ling, A. Sarvaramini et al., "Stabilization of basic oxygen furnace slag by hot-stage carbonation treatment," *Chemical Engineering Journal*, vol. 203, pp. 239–250, 2012.

[25] R. M. Santos, J. Van Bouwel, E. Vandevelde, G. Mertens, J. Elsen, and T. Van Gerven, "Accelerated mineral carbonation of stainless steel slags for CO_2 storage and waste valorization: effect of process parameters on geochemical properties," *International Journal of Greenhouse Gas Control*, vol. 17, pp. 32–45, 2013.

[26] S. Ghoshal and F. Zeman, "Carbon dioxide (CO_2) capture and storage technology in the cement and concrete industry," in *Developments and Innovation in Carbon Dioxide (CO_2) Capture and Storage Technology*, M. Mercedes Maroto-Valer, Ed., vol. 1 of *Woodhead Publishing Series in Energy*, pp. 469–491, Woodhead Publishing, 2010.

[27] Y. Chen, "Research and first application of the CO_2 Capture and Storage (CCS) technology in cement industry," *Cement Guide for New Epoch*, vol. 25, no. 3, pp. 6-7, 95, 2019.

[28] L. Huang, "Application and practice of CO_2 pressure swing adsorption capture technology for cement kiln tail flue gas," *Cement*, vol. 1, pp. 1-2, 2022.

[29] D. Bonenfant, L. Kharoune, S. Sauvé et al., "CO_2 sequestration potential of steel slags at ambient pressure and temperature," *Industrial & Engineering Chemistry Research*, vol. 47, no. 20, pp. 7610–7616, 2008.

[30] Z. Liu and W. Meng, "Fundamental understanding of carbonation curing and durability of carbonation-cured cement-based composites: a review," *Journal of CO_2 Utilization*, vol. 44, Article ID 101428, 2021.

[31] C.-Y. Wang, W.-J. Bao, Z.-C. Guo, and H.-Q. Li, "Carbon dioxide sequestration via steelmaking slag carbonation in alkali solutions: experimental investigation and process evaluation," *Acta Metallurgica Sinica (English Letters)*, vol. 31, no. 7, pp. 771–784, 2018.

[32] X. J. Liang, *Studies on Relationship of Carbonation with Hydration of Steel Slag and Cement*, University of Jinan, Doctoral dissertation, Jinan, 2012.

[33] Z. Yi, T. Wang, and R. Guo, "Sustainable building material from CO_2 mineralization slag: aggregate for concretes and effect of CO_2 curing," *Journal of CO_2 Utilization*, vol. 40, Article ID 101196, 2020.

[34] Y. Fang, S. Wang, Y. Tong, X. Sun, X. Ding, and W. Su, "Effect of carbonation pretreatment on volume stability and hydration activity of steel slag-cement composite cementitious materials," *Bulletin of the Chinese Ceramic Society*, vol. 42, no. 3, Article ID 1001, 2023.